DOI: 10.1002/anie.201101405

Multiferroics

Electric Control of Magnetization and Interplay between Orbital Ordering and Ferroelectricity in a Multiferroic Metal–Organic Framework**

Alessandro Stroppa, Prashant Jain,* Paolo Barone, Martijn Marsman, Juan Manuel Perez-Mato, Anthony K. Cheetham, Harold W. Kroto, and Silvia Picozzi*

Materials that combine magnetic and electrical ordering, that is, multiferroics,[1] are highly desirable for technological applications.[2] Most of the many new multiferroics that have been discovered in the last few years are transition-metal oxides. Very recently, however, the search for new multiferroics and ferroelectrics has been extended to include organic compounds.[3,4] Materials known as metal–organic frameworks (MOFs), crystalline compounds consisting of networks of metal ions connected by coordinating organic linkers, are attracting increasing attention.[5,6] Particularly interesting are MOFs with the perovskite ABX_3 architecture, some of which exhibit multiferroic behavior.[7–10] Because they are hybrid systems, they may benefit from the properties of both the inorganic and organic building blocks from which they are constructed and can therefore show new and interesting properties with novel applications.[11,12] One of the main advantages of magnetic MOFs, compared to inorganic compounds, is the possibility of tuning or controlling the nature of the magnetic coupling that is provided by the variety of possible starting building blocks (metal ions, short ligands, co-ligands, templates, etc.) that can be chosen and assembled into solid-state structures.[13] It is then hoped that in multiferroic MOFs the high tunability can be extended to the control of ferroelectric properties, thus opening up new routes to lead-free compounds exhibiting strong polarization.

Recently, Hu et al. synthesized a series of novel perovskite-like metal formates, that is, $[C(NH_2)_3]M(HCOO)_3$ (M = divalent Mn, Fe, Co, Ni, Cu, and Zn).[6] Among them, the copper-based compound is particularly interesting. It has a polar space group $Pna2_1$ and exhibits spin-canted antiferromagnetism with a Néel temperature of 4.6 K. Hu et al. suggested that this compound should exhibit multiferroic behavior.[6] Recently, some of us reported four metal–organic frameworks, $[(CH_3)_2NH_2]M(HCOO)_3$ (M = Mn, Fe, Co and Ni) that exhibited multiferroic behavior associated with an order–disorder phase transition.[7] Since this discovery, there has been a lot of interest in the field of multiferroic MOFs.[9] However, there have not been any theoretical or computational studies on these systems.

We have carried out ab initio simulations on $[C(NH_2)_3]Cu[(HCOO)_3]$ with the perovskite-like structure ABX_3, where A is $[C(NH_2)_3]^+$, B is the Jahn–Teller-active Cu^{2+} ion, and X is the $HCOO^-$ group. This compound is expected to exhibit ferroelectric behavior and a topology similar to the multiferroic systems some of us reported in the past.[7,8] The unit cell contains four formula units. Hereafter we refer to this compound as Cu-MOF.

The octahedrally coordinated Cu ions are connected by HCOO bridges, forming the ReO_3-type anionic $[Cu(HCOO)_3]$ framework, with the $C(NH_2)_3$ groups in the nearly cubic cavities (Figure 1). The Cu^{2+} ion (d^9 with $t_2^6e^3$ electronic configuration) lies approximately at the center of a distorted octahedron with two short (*s*) and two long (*l*) equatorial Cu–O_{eq} bonds (1.97, 1.99 Å and 2.37, 2.39 Å, respectively) and two medium (*m*) apical Cu–O_{ap} bonds (2.01 and 2.02 Å). The octahedra are tilted about the *c* axis by approximately 20° (Figure 1c). The Cu-MOF can then be viewed as being composed of chains running along the *c* axis; within the chains, the square-planar Cu units are connected by apical $HCO_{ap}O_{ap}$ groups. Parallel chains are connected by equatorial $HCO_{eq}O_{eq}$ groups. The square-planar Cu–O_{eq} units display an antiferro-distortive pattern[14] within the *ab* planes: the elongated axes (defined by the long Cu–O_{eq} bonds) of neighboring square-planar units are almost perpendicular to each other (see Figure 1d), corresponding to an antiferro-orbital ordering[15] on Cu sites, that is, the antiparallel ordering of electronic orbitals.[16] On the other hand, along

[*] Dr. A. Stroppa, Dr. P. Barone, Dr. S. Picozzi
CNR-SPIN, L'Aquila (Italy)
E-mail: alessandro.stroppa@spin.cnr.it
Dr. P. Jain, Prof. H. W. Kroto
Department of Chemistry and Biochemistry, Florida State University
Tallahassee, FL 32306 (USA)
E-mail: pj05c@fsu.edu
Dr. M. Marsman
University of Vienna, Faculty of Physics and Center for Computational Materials Science (Austria)
Prof. J. M. Perez-Mato
Departamento de Fisica de la Materia Condensada
Facultad de Ciencia y Tecnologia, UPV/EHU, Bilbao (Spain)
Prof. A. K. Cheetham
Department of Materials Science and Metallurgy
University of Cambridge (UK)

[**] This research was funded by the European Research Council under the European Community, 7th Framework Programme (2007–2013)/ERC Grant Agreement no. 203523. Computational support by CASPUR Supercomputing Center in Rome through "Standard HPC Grant 2010" is gratefully acknowledged. A.S., P.B., and S.P. wish to thank D. Khomskii for his careful reading of the manuscript and helpful insights. A.S. greatly acknowledges the visiting period at University of the Basque country in Bilbao, where part of this work was carried out, and the warm hospitality of the members of this institute. A.S. thanks F. De Angelis and M. Aschi (University of L'Aquila) for useful discussions. H.W.K. and P.J. thank the FSU Research Foundation for support.

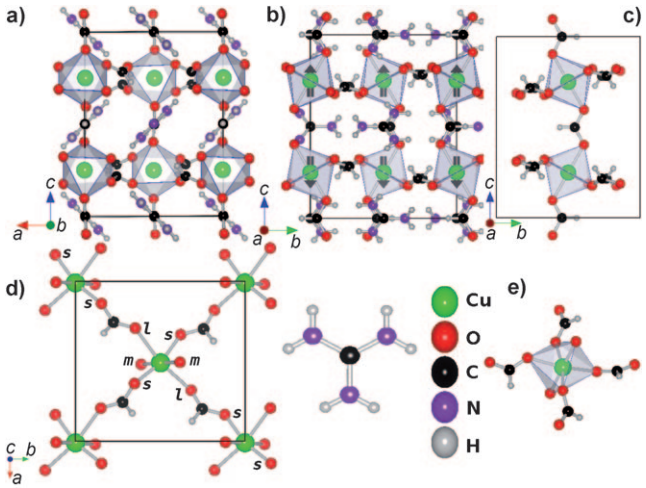

Figure 1. Crystal structure of $[C(NH_2)_3]Cu(HCOO)_3$. a, b) Side views. The octahedra are linked by HCOO groups, while the A sites of the perovskite network are occupied by $C(NH_2)_3$ groups. The spin configuration is represented by arrows at Cu sites. c) A single linear chain (see text) along the *c* polar axis. d) *ab* plane and corresponding long (*l*), short (*s*), and medium (*m*) bond lengths. e) Perspective view of the $C(NH_2)_3$ unit and the octahedra with HCOO groups.

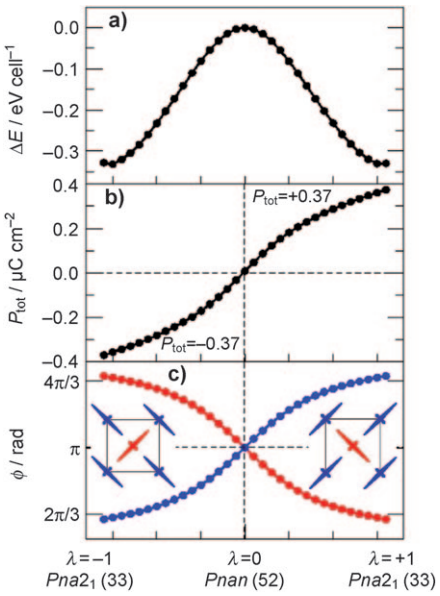

Figure 2. Path connecting the virtual nonpolar and the two polar phases with opposite polarizations. a) Total energy difference with respect to the paraelectric phase. b) The polarization P_{tot} as a function of λ. c) Evolution of the Jahn–Teller phases $\phi = \tan^{-1}Q_2/Q_3$ as a function of λ. Blue and red color refer to the two Cu sublattices with different direction of the elongation axis (*l*) in the *ab* plane.

the chain, the crystal shows a ferro-orbital ordering. This situation is analogous to the behavior of well-studied $KCuF_3$ perovskite.[17] In turn, the orbital order is directly coupled to magnetic exchange interactions. The Goodenough–Kanamori–Anderson (GKA) rules[18] suggest that there is a strong antiferromagnetic coupling if singly occupied orbitals on corresponding sites are directed towards each other. If, however, an occupied orbital is directed towards an empty (or doubly occupied) one, there will be a weaker ferromagnetic coupling. Thus, in our case, the antiferro-orbital ordered planes are coupled ferromagnetically, while they order antiferromagnetically (AFM) in the perpendicular direction, that is, the ground state displays an A-type AFM spin configuration.[19,20] Indeed, the exchange couplings estimated by mapping onto a Heisenberg model ($H = -\Sigma_{ij} J_{ij} S_i S_j$) indicates an AFM intrachain coupling $J_c \approx -44\ cm^{-1}$ and FM (ferromagnetic) interchain coupling $J_a \approx 8\ cm^{-1}$. The stronger AFM intrachain interaction ($|J_c| \gg J_a$) is in agreement with experiments.[6] Note that a small weak ferromagnetic component allowed by symmetry in this compound is supported by SQUID measurements.[6] We discuss this key point below.

To calculate the degree of polarization, we consider a virtual parent high-symmetry structure as a paraelectric phase.[21,22] The presence of the organic groups together with the tilting of the octahedra reduces the likely parent symmetry to the centrosymmetric space group *Pnan* (no. 52). In Figure 2, we correlate the paraelectric structure ($\lambda = 0$) with the ferroelectric structure in polar space group $Pna2_1$ ($|\lambda|=1$) by a linear interpolation of atomic positions as a function of λ. Therefore, the parameter λ is proportional to the amplitude of the polar distortion at a given geometry. The maximum atomic displacement between $\lambda = 0$ and $|\lambda| = 1$ is approximately 0.24 Å, and the polar phase is calculated to be more stable than the nonpolar phase by 0.08 eV molecule^{-1}, a result comparable with the case of $BaTiO_3$. The calculated total energy as a function of λ produces the expected double-well profile characteristic of a switchable ferroelectric system. In Figure 2b, we show the plot of the polarization P_{tot} along the polar axis *c* as a function of λ. The polarization is 0.37 μC cm^{-2} for $\lambda = 1$.

It is interesting to follow the evolution of the antiferro-distortive pattern from the centrosymmetric to the polar phase. The Jahn–Teller coordinate vector with components Q_2, Q_3 is introduced, where $Q_2 = (l-s)/\sqrt{2}$, $Q_3 = (2m-l-s)/\sqrt{6}$, where *l*, and *s* refer to the lengths of the long and short bonds, respectively, in the *ab* planes and *m* to the lengths of the Cu–O_{ap} bonds. Clearly, a larger modulus ρ of this vector results in a larger distortion from octahedral symmetry. In the antiferro-distortive pattern at $\lambda = +1$, two sublattices can be distinguished (Figure 2c): one with elongated axis along [1,1,0] (blue), the other along $[\bar{1},1,0]$ (red). By introducing the polar coordinates[14] as $Q_2 = \rho\sin\phi$, $Q_3 = \rho\cos\phi$, where $\phi = \tan^{-1}Q_2/Q_3$ is the so-called Jahn–Teller phase,[15,14] the antiferro-distortive pattern can be monitored by the changes in ϕ. For $\lambda = 1$ (positive polarization), $\phi \approx 4\pi/3$ for the octahedra elongated along [1,1,0] (blue) and $\phi \approx 2\pi/3$ for octahedra elongated along $[\bar{1},1,0]$ (red). For $\lambda = -1$ (negative polarization), the two octahedral sublattices interchange the direction of the elongated axis (Figure 2c) and, at the same time, the value of the Jahn–Teller phase. The antiferro-distortive pattern disappears in the $\lambda = 0$ (centrosymmetric) phase, that is, $\phi = \pi$, $Q_2 = 0$, and $l = s$. The parallel behavior of ϕ and of the polarization as a function of λ clearly indicate that ferroelectricity and antiferro-distortive modes (and related orbital order) are correlated. Note that the two antiferro-distortive patterns are centrosymmetric (Figure 2c).

It is remarkable that although the Jahn–Teller local modes are nonpolar, the correlated antiferro-distortive Jahn–Teller effect is sufficient to break the inversion symmetry by coupling through hydrogen bonding to additional atomic displacements of the A group, responsible for the polarization, as explained below. Here, the Jahn–Teller effect and related orbital order drive the ferroelectric properties of this phase.

Our study has revealed an important property of the Cu-MOF. Depending on the direction of the spins of the A-type AFM ordering, a weak ferromagnetic component should be induced by the polar distortion. Furthermore, the magnetic space groups resulting from the AFM ordering are $Pna'2_1'$ and $Pn'a'2_1$ for AFM spins directed along the c and a axes, respectively. These symmetries allow ferromagnetic ordering along the a and c axes, respectively, and indeed, a weak ferromagnetic component in these directions, induced by symmetry couplings of type $M_aP_cLA_c$ and $M_cP_cLA_a$, respectively, is to be expected. Here, LA is the magnitude of the AFM-A ordered spin. Therefore, for a constant AFM ordering, a secondary FM component is induced approximately proportional to the polarization and, most importantly, switchable with it. For a fixed orientation of the AFM ordering of, for example, spins lying along the c direction, the variation of the magnetic ordering was calculated as a function of the amplitude of the polar distortion. Cu magnetic moments were found to have a secondary FM component along the a direction. Figure 3 shows the variation of this component with the amplitude of the polar distortion and the resulting correlation with the electric polarization. Calculation indicates approximately linear dependence of the FM component on the electric polarization and the expected switch of sign for the two equivalent ferroelectric domains. Hence, an electric field along the c axis, which would switch the spontaneous polarization, would, at the same time, switch the sign of M_a. This behavior indicates that Cu-MOF should exhibit control of magnetization by an electric field, a long-sought property with exciting technological applications.

In Figure 4, we show the hydrogen bond (dashed line) connecting the H atoms of the A group with the nearest O_{eq}

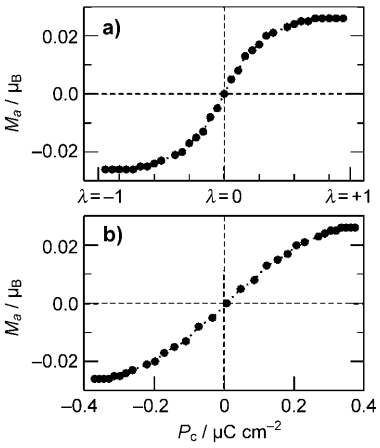

Figure 3. Electrical control of magnetization. a) Weak FM component as a function of the polar distortion and b) as a function of the polarization.

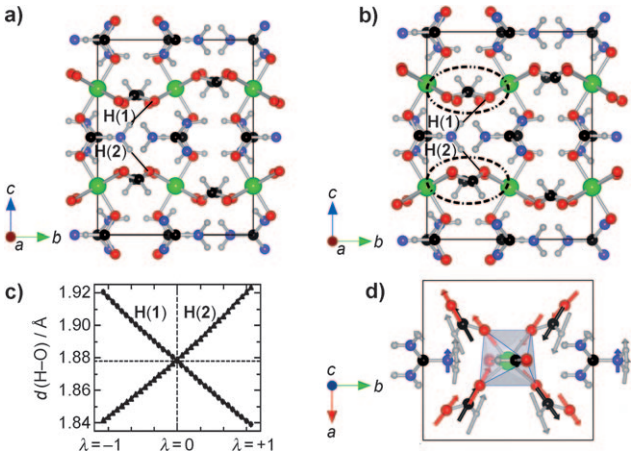

Figure 4. Coupling of the Jahn–Teller modes to A-group atoms through hydrogen bonding. a) Side view: hydrogen bonding in the centrosymmetric phase. b) Side view: hydrogen bonding in the polar phase. Dashed ellipses highlight the asymmetry of the environment of the NH_2 of the A cation. c) Evolution of the H···O_{eq} distances as a function of the polar distortion (see text for details). d) Top view: characteristic displacements of the Q_2 Jahn Teller mode.

atom of the Cu octahedra in the paraelectric (Figure 4a) and ferroelectric (Figure 4b) phase. In Figure 4d, the arrows represent the atomic displacements of the octahedra and neighboring A cations from the paraelectric to the polar structure. The characteristic pattern of Jahn–Teller displacements of the $HCO_{eq}O_{eq}$ groups is readily recognizable. The largest displacements in the A cation correspond to H(1) and H(2), which clearly "follow" the Q_2 Jahn–Teller mode (Figure 4d). Note that in the centrosymmetric phase, the distances H···O_{eq}, that is, d(O–H(1)) and d(O–H(2)), are equal (Figure 4c). For positive λ, the former decreases and the latter increases (and vice versa for negative λ). Therefore, the correlated in-plane Jahn–Teller modes are linearly coupled to the NH_2 atoms of A-group atoms through hydrogen bonds. The displacements of the NH_2 group of the A cation give rise to small induced dipole moments, which, in turn, sum up to a net component along the c axis, resulting in an out-of-plane ferroelectric polarization. To confirm this mechanism, we have displaced only the atoms of the A group from the centrosymmetric to the polar phase. The resulting polarization is estimated to be approximately 0.21 μC cm^{-2}, more than half of the total polarization previously reported. On the other hand, if we displace only the atoms of the BX_3 groups and keep the A-group atoms at their centrosymmetric positions, the polarization is almost zero. This result shows unambiguously that, as expected, the Jahn–Teller distortion modes do not contribute to the polarization and that the A-group atoms are the main source of polarization. If the A-group atoms are allowed to relax, the true polar state is recovered, that is, all the atoms return to their position in the $\lambda = 1$ structure. The mechanism of polarization also suggests that using a different A cation with more polarizable electron density would increase the polarization.

In summary, our study shows that the Cu-MOF should be a new multiferroic metal–organic framework, in which the Jahn–Teller and antiferro-distortions cooperate to induce a

switchable ferroelectric polarization by coupling to the A-group atoms through hydrogen bonding. Most importantly, a weak ferromagnetic component (M_a) is coupled to the spontaneous polarization (P_c), and they are mutually reversible. Thus, our results show that Cu-MOF should exhibit weak ferromagnetism coupled with ferroelectricity, a rare phenomenon. It should be a true magnetoelectric multiferroic, first proposed by Fox and Scott,[23] thus making this material very attractive for advanced memory devices. Although the predicted polarization is small, the rich variety of modifications possible in this class of MOFs, for example, by alteration of organic ligand, template, and strain, opens up new avenues in the exciting field of multiferroics.

Methods

All calculations were performed with the Vienna Ab initio Simulation Package (VASP),[24] using the projector augmented-wave (PAW) method[25] with the Perdew–Burke–Ernzerhof (PBE) GGA functional.[26] The energy cutoff was set to 400 eV and a $2\times4\times4$ Monkhorst-Pack grid of k points was used. The Berry phase approach[27] was employed to calculate the ferroelectric polarization P. We also used the Heyd–Scuseria–Ernzerhof hybrid functional (HSE),[28] which mixes a fraction of Fock exchange with the exchange density functional. This method improves the theoretical description of solids.[29–31] As we are dealing with weak bonds, we also benchmarked our calculations with an empirical method to account for van der Waals interactions in density functional theory calculations, called Grimme's corrections[32] and implemented in VASP by T. Bucko.[33] Figures were plotted using the VESTA package.[34]

Received: February 25, 2011
Published online: May 25, 2011

Keywords: hydrogen bonding · Jahn–Teller effect · magnetoelectricity · metal–organic frameworks · multiferroics

[1] W. Eerenstein, N. D. Mathur, J. F. Scott, *Nature* **2006**, *442*, 759.
[2] S. W. Cheong, M. Mostovoy, *Nat. Mater.* **2007**, *6*, 13.
[3] G. Giovannetti, S. Kumar, A. Stroppa, J. van den Brink, S. Picozzi, *Phys. Rev. Lett.* **2009**, *103*, 266401.
[4] S. Horiuchi, Y. Tokunaga, G. Giovannetti, S. Picozzi, H. Itoh, R. Shimano, R. Kumai, T. Yoshinori, *Nature* **2010**, *463*, 789.
[5] Q. Ye, D.-W. Fu, H. Tian, R.-G. Xiong, P. W. H. Chan, S. D. Huang, *Inorg. Chem.* **2008**, *47*, 772.
[6] K.-L. Hu, M. Kurmoo, M. Wang, S. Gao, *Chem. Eur. J.* **2009**, *15*, 12050.
[7] P. Jain, N. S. Dalai, B. H. Toby, H. W. Kroto, A. K. Cheetham, *J. Am. Chem. Soc.* **2008**, *130*, 10450.
[8] P. Jain, V. Ramachandran, R. J. Clark, H. D. Zhou, B. H. Toby, N. S. Dalai, H. , W. Kroto, A. K. Cheetham, *J. Am. Chem. Soc.* **2009**, *131*, 13625.
[9] R. Ramesh, *Nature* **2009**, *461*, 1218.
[10] M. Sánchez-Andújar, S. Presedo, S. Vanez-Vilar, S. Castro-Garcia, J. Shamir, M. A. Senaris-Rodriguez, *Inorg. Chem.* **2010**, *49*, 1510.
[11] A. K. Cheetham, C. N. R. Rao, *Science* **2007**, *318*, 58.
[12] C. N. R. Rao, A. K. Cheetham, A. Thirumurugan, *J. Phys. Condens. Matter* **2008**, *20*, 083202.
[13] V. S. Zapf, M. Kenzelmann, F. Wolff-Fabris, F. Balakirev, Y. Chen, *Phys. Rev. B* **2008**, *82*, 1.
[14] I. Bersuker, *The Jahn–Teller Effect*, Cambridge University Press, Cambridge, **2006**.
[15] D. I. Khomskii, *Phys. Scr.* **2005**, *72*, CC8.
[16] M. Kataoka, *J. Phys. Soc. Jpn.* **2001**, *70*, 2353.
[17] M. Towler, R. Dovesi, V. S. Saunders, *Phys. Rev. B* **1995**, *52*, 10150.
[18] J. B. Goodenough, *Magnetism and Chemical Bond*, Interscience Publ., New York, **1963**; "Electronic structure, exchange and magnetism in oxides": D. J. Khomskii in *Spin Electronics* (Eds.: M. Ziese, M. J. Thornton), Springer, Berlin, **2001**.
[19] G. E. Bacon, *Neutron Diffraction*, Oxford University Press, Oxford, **1962**.
[20] E. O. Wollan, W. C. Koehler, *Phys. Rev.* **1955**, *100*, 545.
[21] D. Orobengoa, C. Capillas, M. I. Aroyo, J. M. Perez-Mato, *J. Appl. Crystallogr.* **2009**, *42*, 820.
[22] E. Kroumova, M. I. Aroyo, J. M. Perez-Mato, S. Ivantchev, J. M. Igartua, H. Wondratschek, *J. Appl. Crystallogr.* **2001**, *34*, 783.
[23] D. L. Fox, J. F. Scott, *J. Phys. C* **1977**, *10*, L329.
[24] G. Kresse, J. Furthmüller, *Phys. Rev. B* **1996**, *54*, 11169.
[25] P. E. Blöchl, *Phys. Rev. B* **1994**, *50*, 17953.
[26] J. P. Perdew, K. Burke, M. Ernzerhof, *Phys. Rev. Lett.* **1996**, *77*, 3865.
[27] R. D. King-Smith, D. Vanderbilt, *Phys. Rev. B* **1993**, *47*, 1651.
[28] J. Heyd, G. E. Scuseria, M. Ernzerhof, *J. Chem. Phys.* **2003**, *118*, 8207.
[29] J. Paier, R. Hirschl, M. Marsman, G. Kresse, *J. Chem. Phys.* **2005**, *122*, 234102.
[30] A. Stroppa, S. Picozzi, *Phys. Chem. Chem. Phys.* **2010**, *12*, 5405.
[31] W. F. Perger, *Chem. Phys. Lett.* **2003**, *368*, 319.
[32] S. Grimme, *J. Comput. Chem.* **2004**, *25*, 1463.
[33] T. Bučko, J. Hafner, S. Lebègue, J. G. Ángyán, *J. Phys. Chem. A* **2010**, *114*, 11814.
[34] K. Momma, F. Izumi, *J. Appl. Crystallogr.* **2008**, *41*, 653.

